Role of sulfur in BaVS3 probed by S K-edge absorption spectroscopy

Vita Ilakovac, S. Boulfaat, Yves Joly, A.M. Flank, P. Lagarde, M. Žitnik, M. Fialin, H. Berger, L. Forró

Physica B

Role of sulfur in $BaVS_3$ probed by S K-edge absorption spectroscopy

V. Ilakovac[a,b,c,*], S. Boulfaat[a,b], Y. Joly[d,e], A. M. Flank[f], P. Lagarde[f], M. Žitnik[g], M. Fialin[h], H. Berger[i], L. Forró[i]

[a] *Sorbonne Universités, UPMC Univ Paris 06, UMR 7614, LCP-MR, F-75005, Paris, France*
[b] *CNRS, UMR 7614, LCP-MR, F-75005, Paris, France*
[c] *Université de Cergy-Pontoise, F-95031 Cergy-Pontoise, France*
[d] *Université Grenoble Alpes, Institut NEEL, F-38000 Grenoble, France*
[e] *CNRS, Institut NEEL, F-38042 Grenoble, France*
[f] *Synchrotron SOLEIL, St. Aubin, France*
[g] *Institut Jožef Štefan, Ljubljana, Slovenia*
[h] *CAMPARIS, UPMC, IPGP, Paris, France*
[i] *ICPM, Ecole Polytechnique Fédérale de Lausanne, Switzerland*

Abstract

We show that the quasi-1D behavior of $BaVS_3$ can be understood analyzing the X-ray absorption near edge spectra at the sulfur K edge. Linear dichroïsm experiments, analyzed with the help of *ab initio* calculations, reveal two strong and polarization dependent pre-edge features, induced by the band character of the 3*d* vanadium levels. They are related to crystal field split t_{2g} and e_g states. When the temperature is lowered, the t_{2g} feature shifts progressively to higher energy, and its intensity increases for the polarization along the *c*-axis, stacking direction of the V-S face sharing octahedra. This behavior points to the depletion of sulfur states and thus the lack of S 3*p* - V 3*d* hybridization in the direction of V-S chains.

Keywords: Metal-insulator transitions and other electronic transitions, X-ray absorption spectroscopy, Charge-density-wave system

1. Introduction

Understanding the interaction of itinerant and localized electrons is one of main challenges in solid state sciences. It determines properties of a large class of correlated systems with very rich phase diagrams, involving a subtle interplay between charge, orbital, and spin degrees of freedom [1]. The complex electronic structure of $BaVS_3$, in spite of its apparently simple quasi-1D geometry, ranks it among model compounds for the study of the competition of different ordering parameters.

$BaVS_3$ structure is constituted of chains of V-S face sharing octahedra running in *c*-direction and separated by Ba atoms [2]. The distance between neighboring V atoms along the V-S chains is less than two times shorter then the one between the chains. It could thus be considered as a quasi-1D compound. Nevertheless, its conductivity anisotropy is extremely low compared to usual quasi-1D compounds [3]. It undergoes three low temperature second order transitions. In stoichiometric $BaVS_3$, they occur at 240 K, 69 K and 30 K. The first is related to a structural change, a zigzag deformation of the V-S chains, reducing the crystal symmetry from hexagonal to orthorhombic, without altering its paramagnetic and conducting properties [2]. The metal-insulator (MI) transition at T_{MI} = 69 K is accompanied by the doubling of the unit cell in the *c* direction [4]. The pre-transitional diffuse lines, observed at the wave-vector $q_{MI} = 0.5\ c^*$ in x-ray diagrams, reveal the formation of the charge density waves (CDW) in V-S chains already at 170 K [5]. It is surprising that only half of active electrons directly participate to the $2k_F$ Peierls instability. Spin degrees of freedom are affected at the MI

*Corresponding author: vita.ilakovac-casses@upmc.fr

transition [3], but freeze only below the Néel temperature, T_N = 30 K, establishing an incommensurate antiferromagnetic (AF) order in the (a, b) plane, as determined by the inelastic neutron scattering measurements on powder samples [6]. The third component of the AF incommensurability is brought to light by single crystal resonant X-ray diffraction at the V L_3 edge, refining the ordering wave vector q_{AF} = (0.226, 0.226, 0.016) [7, 8]. Moreover, these measurements reveal that the spins are polarized along the a direction and ordered alternatively in the b direction of the lowest temperature (monoclinic) unit cell. A conical spin arrangement could explain the incommensurate order along V-S chains [9].

Local density approximation (LDA) calculations reveal an interplay between two different types of t_{2g} electron states at the Fermi level: two narrow $e(t_{2g})$ bands, and one dispersive band with mainly d_{z^2} character, related to delocalized states directed along the V-S chains [10, 11, 12]. They are occupied by a single $3d^1$ electron of the formally V^{4+} ion. However, according to the LDA, the delocalized d_{z^2} states are nearly completely filled, which overestimates the itinerant character and fails to explain the gap opening in the insulating phase. LSDA + U calculations, including a static exchange and an antiferromagnetic ordering in the (a,b) plane, find a 0.15 eV gap but do not explain the paramagnetism in the metallic phase [13]. The experimental 1:1 filling ratio of the $d_{z^2}/e(t_{2g})$ states and the gap opening in the insulating phase are correctly reproduced when the correlation and exchange effects are included via dynamical mean field theory (DMFT) [14].

Already in earliest studies, it was shown that the sulfur content is determinant for $BaVS_3$ properties. Massenet et al. [16] report lowering of the T_S down to 150 K and ferromagnetic behavior below 16–17 K in $BaVS_{3-\delta}$ with δ = 0.12. More systematic study of magnetization, conductivity and NMR measurements are performed with a formal δ = 0.05, 0.10, 0.15 and 0.20 [17]. The deficiency of about (nominal) 3 % turns $BaVS_{3-\delta}$ to paramagnetic semiconductor already at room temperature. A short range 3D charge order (CO) at the wave vector q_{CO} = (2/3, 0, ≈ 1/5)$_O$ exists already at 300 K. Quasi-1D Peierls instability is suppressed. Instead, a long range order develops at q_{CO} below 110-220 K [18, 19]. The work of Yamasaki et al. [17] confirms that below 15–18 K the sulfur deficient $BaVS_{3-\delta}$ becomes a ferromagnet.

X-ray absorption near edge spectroscopy (XANES) is an experimental tool which is able to give relevant information on both structural and electronic aspects of a studied system. The full power of this spectroscopy is used when the polarization analysis is applied on a single crystal material, as the selection rules permit to probe particular electronic states. The purpose of this paper is to show that such experiments combined with the *ab–initio* simulations reveal subtle details of the electronic structure of $BaVS_3$ in different phases of the compound. The originality of the work is in performing the measurements at the S K edge, a priory probing S $3p$ states, while gaining insight into relative (de)localisation of V $3d$ – S $3p$ overlap.

The details of the realized S K edge polarization and temperature dependent XANES experiment on $BaVS_3$ and accompanying calculations are presented in the section 2. They are followed by the presentation of results and their interpretations in section 3 and 4, respectively.

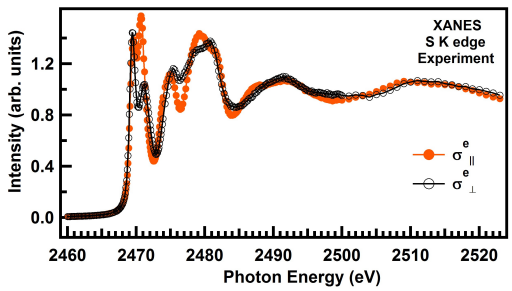

Figure 1: S K edge XANES of $BaVS_3$ measured for $\epsilon \parallel c$ ($\sigma^e_\parallel$, orange cercles) and $\epsilon \perp c$ ($\sigma^e_\perp$, black points). Superscript e stands for experiment.

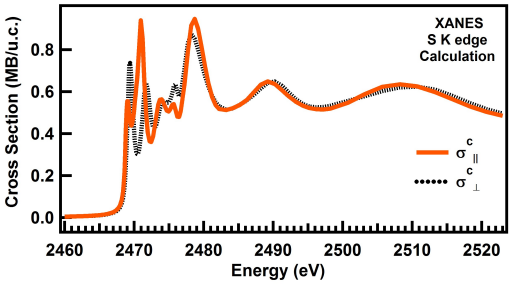

Figure 2: Calculated S K edge cross section of $BaVS_3$ in Mbarn per unit cell for $\epsilon \parallel c$ ($\sigma^c_\parallel$, orange line) and $\epsilon \perp c$ ($\sigma^c_\perp$, black dotted line). Superscript c stands for calculation.

2. Experiment and calculation details

Single crystal $BaVS_3$ samples are grown by the tellurium flux method [20]. Strong polarization dependence of the S K edge x-ray absorption spectra at room temperature (measured in the fluorescence mode) was

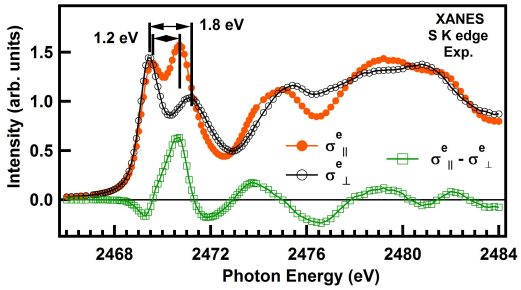

Figure 3: Polarization dependence in the near S K edge region. The difference of the intensities, $\sigma^e_{\parallel}$ - $\sigma^e_{\perp}$, the linear dichroïsm, is shown by green squares.

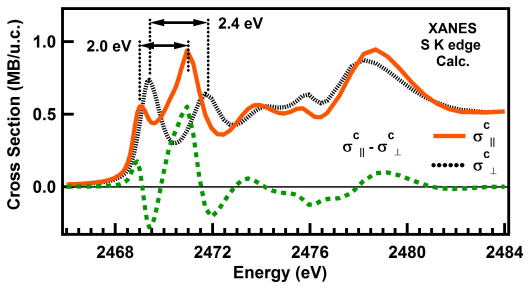

Figure 4: Calculated near S K edge spectra for $\epsilon \parallel c$ (orange line) and $\epsilon \perp c$ (black dotted line). Linear dichroïsm, $\sigma^c_{\parallel}$ - $\sigma^c_{\perp}$, is presented by the green dotted line.

observed at the ID26 beamline at ESRF. The temperature dependence was further studied at the LUCIA beamline (SOLEIL). Two samples from the same batch were mounted on a closed circle He cryostat with their needle axis (c crystal axis) either parallel or perpendicular to the scattering plane. Microsonde analysis on a SX100 CAMECA performed with 20 kV accelerated electrons did not show any notable difference in the composition of the two samples. The incident light was normal to the sample surface and polarized in the scattering plane. The two sample geometries permitted us to study two orientations relative to the incoming light polarization : $\epsilon \parallel c$ and $\epsilon \perp c$. The intensity of the fluorescence was measured in a total yield mode by a detector at 90° scattering angle. The inflection point of the S edge of the pure sulfur was at 2472 eV with the energy resolution of 0.3 eV. The normalization and the self-absorption correction of the spectra are performed by a code using the procedure described in ref.[21, 22].

Calculations of the room temperature spectra are performed by the Finite Difference Method Near Edge Spectroscopy (FDMNES) code [23] in the LSDA+U frame. Prior to the evaluation of the cross section, the Schrödinger equation is resolved by the finite difference method in the excited state of a 6 Å cluster embedded in a hexagonal phase $BaVS_3$.

3. Results

Room temperature $BaVS_3$ S K edge XANES spectra in Fig. 1 show a very strong pre-edge doublet at 2468–2472 eV, a large structured edge feature at 2472–2484 eV and two extended structures at higher energy. The difference between the $\epsilon \parallel c$ and $\epsilon \perp c$ spectra is particularly strong in the pre-edge and the edge region, and becomes less important, but still existent at higher energy. We keep the pre-edge terminology because these features, often present in the S or O K-edges in metallic oxides or sulfides appear at lower energy than the corresponding edge in pure compounds.

FDMNES calculations reproduce all the features in the experimental spectra (see Fig. 2). There are however small differences in relative positions and shapes. In particular, the extended structures are slightly shifted to lower energy and the edge structure at 2480 eV is not as large as the experimental one.

The pre-edge and the edge region (2468–2484 eV) is enlarged in Fig. 3. The polarization dependence is here much more evident compared to the spectra collected at the V L edge [25]. It is worth to note that V L edge x-ray absorption spectroscopy probes V $3d$ states directly via dipolar transition rules, while S K edge XANES gives only an indirect insight, through V $3d$ – S $3p$ hybridization. The polarization dependence is particularly important in the region of the second pre-edge peak (2469.2 eV), where $\sigma^e_{\parallel}$ is much stronger compared to $\sigma^e_{\perp}$ (e stands for experiment). Moreover, the energy difference between the two pre-edge features, is not the same for the two geometries: $\Delta^e_{\parallel} = 1.2$ eV, while $\Delta^e_{\perp} = 1.8$ eV. The difference of the two spectra ($\sigma^e_{\parallel} - \sigma^e_{\perp}$), the linear dichroïsm, is shown in the same figure.

Fig. 4 shows the simulated spectra in the same energy range. The energy difference of the pre-edge peaks is ≈ 50 % larger compared to the experiment, as $\Delta^c_{\parallel} = 2.0$ eV and $\Delta^c_{\perp} = 2.4$ eV (c stands for calculation). Including electron-electron interaction of 5 eV on V– and 2 eV on S–sites improves relative intensities. It induces a partial spectral weight transfer from 2472 eV to 2476 eV and modifies the pre-peak region for $\epsilon \parallel c$. However, it does not modify the relative shift of the two pre-edge features: Δ is not related to the correlation gap. Decreasing the effective core-hole screening to 0.5 elec-

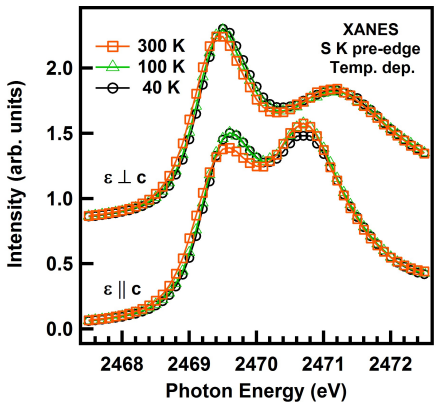

Figure 5: Temperature dependence of the two pre-edge features for the two orientations, $\epsilon \parallel c$ and $\epsilon \perp c$, shifted vertically for clarity.

trons (transition state method with fractional occupation [24]) increases the two peaks in the pre-edge region, in particular the first peak for $\epsilon \parallel c$. It is interesting to note that the calculated $\epsilon \parallel c$ spectra are much more dependent on the cluster size compared to the $\epsilon \perp c$ spectra, indicating that they probe more delocalized states.

The difference of the calculated spectra, $\sigma^c_{\parallel}$ - $\sigma^c_{\perp}$, is presented by the green line in Fig. 4. It matches well the experimental linear dichroïsm except in two points. First, at the very beginning of the pre-edge, the experiment shows no dichroïsm, while the calculated $\sigma^c_{\parallel}$ is more intense than $\sigma^c_{\perp}$. Second, the experiment shows positive dichroïsm at 2482 eV, while the calculations predict slightly negative value. The first discrepancy can be explained by the inability of the LDA based methods to describe correctly the relative occupation of the states at the Fermi level. The second difference can be related to a slight difference of the amount of the sulfur oxide at the surface of the two samples.

The temperature dependence of the two pre-edge structures is shown in Fig. 5. For both orientations, the first pre-edge structure shifts progressively to higher energy as the temperature is lowered. From 300 K to 40 K, the total shift is $\approx$ 80 meV. Moreover, for $\epsilon \parallel c$, the first pre-edge structure increases in intensity for $\approx$ 8% as the temperature is lowered from 300 K to 100 K and remains constant below.

4. Discussion

Pre-edge structures in ligand K-edge spectra of transition metal compounds are often related to mixing of metal-ligand unoccupied states close to the Fermi level. In the case of $BaVS_3$, V $3d$ states overlap with S $3p$ states.

To understand the polarization dependence, we use Cartesian coordinates (x, y, z) with z along the c crystal axis. At the S K edge, quadrupolar transitions are negligible. Thus, when the polarization is along x, y, z, we probe respectively unoccupied $3p_x$, $3p_y$, $3p_z$ sulfur states. Moreover, in the hexagonal phase of $BaVS_3$, the 3-fold axis makes that in the dipole approximation, the absorption signal is isotrope when the polarization is parallel to the basal (x,y) plane, so we can distinguish only $\epsilon \parallel z$ and $\epsilon \perp z$ orientations. Fig. 6 illustrates the relation between S $3p$ and V $3d$ orbitals in V-S octahedra. The point group of vanadium is D_{3d}. Two of its $3d$ orbitals corresponding to e_g representation have lobes pointing to sulfur atoms are shifted to higher energy by the crystal field splitting (upper panel). Other two, $e(t_{2g})$, point to the faces of the V-S octahedra, similarly to d_{z^2} states, and are shifted to lower energy (lower panel).

The S $3p$ and V $3d$ projected density of states (DOS) calculated by FDMNES is shown in Fig. 7. Similarly to the DOS calculations published previously [10, 13, 15] S $3p$ states are strong in the occupied part, while in the unoccupied part V $3d$ predominates. V $3d$ unoccupied DOS is increased at E-$E_F \approx 0$ eV, 1 eV, and 1.8-2.8 eV. The first increase corresponds to d_{z^2} and $e(t_{2g})$ states at the Fermi level, the second to the d_{z^2} free-electron parabola and the third to e_g states.

S $3p$ DOS is increased at energies where V $3d$ states have important density showing that their hybridization is strong. In e_g region, the S $3p_z$ DOS is important at 1.8 eV, while S $3p_{x,y}$ has its maximum at 2.7 eV. This can explain the difference in the pre-edge energy splitting, $\Delta^e_{\parallel}$ ($\Delta^e_{\perp}$) of 1.2 eV (1.8 eV), respectively, even if the calculated values are overestimated. The crystal field splitting is differently probed by $\epsilon \parallel z$ and $\epsilon \perp z$ polarization. On the other hand, the low S $3p_{x,y}$ DOS at E-$E_F \approx 1$ eV indicates that d_{z^2} mixes mostly with the S $3p_z$ states. The S $3p_z$–V $3d_{z^2}$ hybridization is thus the main factor of the quasi-1D behavior of $BaVS_3$.

Contrary to the polarization dependence which is very strong, the temperature variation of the spectra in Fig. 5 is relatively small. For both geometries, the first pre-edge feature shifts to $\approx$ 80 meV higher energy, when the temperature is lowered from 300 K down to 40 K. This value is large compared to the 42 – 70 meV charge gap opening in V $3d$ states below T_{MI} [3, 26, 27, 28, 29, 30]. The shift is progressive, as for 200 K (not shown), its value is in between these measured at 300 K and 100 K. Indeed, at T_S = 240 K, $BaVS_3$ exhibits a hexagonal to orthorhombic second-

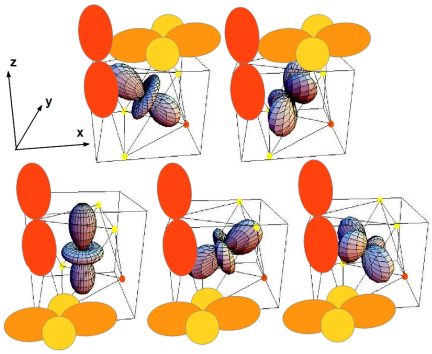

Figure 6: Schematic presentation of V 3d and S 3p electronic states in the room temperature phase. Five V 3d states, two e_g (upper panel), d_{z^2} and two $e(t_{2g})$ (lower panel), are centered on V atoms. S $3p_{x,y}$ (yellow lobes) and S $3p_z$ (orange lobes) are centered on one of six S atoms at the edge of V-S octahedra, stacked along the z-direction. Below T_S, V atoms are displaced out of the center of the octahedra, alternatively in positive (negative) x-direction. Contrary to the hexagonal phase, were all S atoms are equivalent by symmetry, in the orthorhombic phase, there are two types of sulfur atoms, S_1, in the (x,z) plane (orange points), and two S_2 (yellow points), per octahedra.

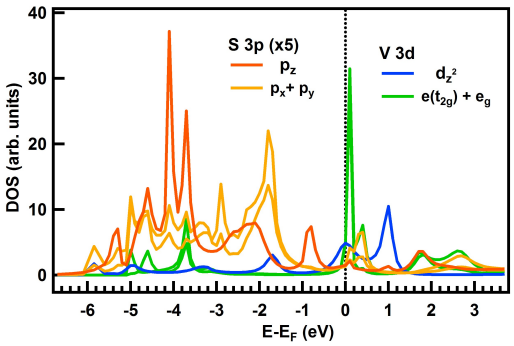

Figure 7: S 3p and V 3d projected DOS of $BaVS_3$. Sulfur DOS is multiplied by five in order to be more evident in the unoccupied part.

order transition. The temperature evolution of cell parameters indicates that the orthorhombic distortion progressively increases when the temperature is lowered [31]. It does not affect remarkably the conducting properties immediately at T_S [3], but it induces a degeneracy break of the two $e(t_{2g})$ states. One of them shifts to 100 meV higher energy (at 100 K), while the other hybridizes strongly with d_{z^2} states [15]. The depletion of V 3d states with strong DOS the Fermi level, reflects in the S K edge XANES as a high energy shift of the first pre-edge peak.

The first pre-edge structure as well increases in intensity for $\epsilon \parallel c$, when the temperature is lowered. This effect is related to the decrease of the S $3p_z$ - V $3d_{z^2}$ hybridization, induced by the zig-zag deformation of vanadium chains. Together with the formation of charge density waves in chains in the pretransitional range ($2k_F$ fluctuations below 170 K), it can induce semiconducting behavior already at 130 K, the temperature which is far above the 69 K MI transition [32].

5. Conclusion

$BaVS_3$ has attracted strong scientific interest since more than forty years, first for its mixed 1D and 3D behavior, and now as a model compound for the study of the localized/itinerant states' interplay. Its properties still hide mysteries, in particular the question of the semiconducting behavior onset above the metal-insulator transition, and the extreme dependence of its properties on the sulfur content. This work combines S K edge x-ray absorption near edge spectroscopy (XANES) and *ab initio* calculations in order to provide original data on the relation between sulfur and vanadium electronic states inside V-S chains. S K-edge XANES measurements reveal two strong and polarization dependent pre-edge structures, related to S 3p and V 3d crystal field split, t_{2g} and e_g, states. The first feature shifts progressively to $\approx$ 80 meV higher energy when the temperature is lowered from 300 K (metallic state) to 40 K (insulating phase). Moreover, when the incoming light polarization is parallel to the c-crystal axis, its intensity increases. This behavior is interpreted by the progressive depletion of S $3p_z$ - V $3d_{z^2}$ hybridization due to the zig-zag deformation of V-S octahedra chains.

6. Acknowledgments

Discussions with N. Trcera, Ph. Sainctavit, R. Nemeusat and D. Cabaret are gratefully acknowledged.

References

[1] M. Imada, A. Fujimori, and Y. Tokura, Rev. Mod. Phys. 70 (1998) 1039
[2] R. Gardner, M. Vlasse and A. Wold, Acta Crystallogr. B 25 (1969) 781
[3] G. Mihály, I. Kézsmárki, F. Zámborszky, M. Miljak, K. Penc, P. Fazekas, H. Berger and L. Forró, Phys. Rev. B 61 (2000) R7831
[4] T. Inami, K. Ohwada, H. Kimura, M. Watanabe, Y. Noda, H. Nakamura, T. Yamasaki, M. Shiga, N. Ikeda and Y. Murakami, Phys. Rev. B 66 (2002) 073108
[5] S. Fagot, P. Foury-Leylekian, S. Ravy, J.-P. Pouget and H. Berger, Phys. Rev. Lett. 90 (2003) 196401

[6] H. Nakamura, T. Yamasaki, S. Giri, H. Imai, M. Shiga, K. Kojima, M. Nishi, K. Kakurai and N. Metoki, J. Phys. Soc. Japan 69 (2000) 2763
[7] Ph. Leininger, V. Ilakovac, Y. Joly, E. Schierle, E. Wesche, O. Bounau, H. Berger, J.-P. Pouget and P. Foury-Leylekian, Phys. Rev. Lett. 106 (2011) 167203
[8] R. A. de Souza, U. Staub, V. Scagnoli, M. Garganourakis, Y. Bodenthin and H. Berger, Phys. Rev. B 84 (2011) 014409
[9] P. Foury-Leylekian, Ph. Leininger, V. Ilakovac, Y. Joly, S. Bernu, S. Fagot and J.-P. Pouget, Physica B 407 (2012) 1692
[10] L. Mattheiss, Solid State Commun. 93 (1995) 791
[11] M.-H. Whangbo, H.-J. Koo, D. Dai and A. Villesuzanne, J. Solid State Chem. 165 (2002) 345
[12] M. Nakamura, A. Sekiyama, H. Namatame, A. Fujimori, H. Yoshihara, T. Ohtani, A. Misu and M. Takano, Phys. Rev. B 49 (1994) 16191
[13] X. Jiang and G. Y. Guo, Phys. Rev. B 70 (2004) 035110
[14] F. Lechermann, S. Biermann and A. Georges, Phys. Rev. Lett. 94 (2005) 166402
[15] F. Lechermann, S. Biermann and A. Georges, Phys. Rev. B 76 (2007) 085101
[16] O. Massenet, R. Buder, J. J. Since, C. Schlenker, J. Mercier, J. Kleber, and D. G. Stucky, Mat. Res. Bu. Vol. 13 (1978) 187
[17] T. Yamasaki, H. Nakamura, M. Shiga , J. Phys. Soc. Japan 69 (2000) 3068
[18] S. Bernu, P. Foury-Leylekian, J.-P. Pouget, A. Akrap, H. Berger, L. Forró, G. Popov, M. Greenblatt, Physica B, 403 (2008) 1625
[19] S. Bernu, P. Foury-Leylekian, P. Fertey, F. Licci, A. Gauzzi, A. Akrap, H. Berger, L. Forró, and J.-P. Pouget, E. Phys. Lett., 89 (2010) 27006
[20] H. Kuriyaki, H. Berger, S. Nishioka, H. Kawakami, K. Hirakawa and F. A. Lévy, Synth. Met. 71 (1995) 2049
[21] D. Manuel, PhD thesis, P. and M. University, Paris, France, 2013
[22] D. Manuel, D. Cabaret, Ch. Brouder, Ph. Sainctavit, A. Bordage, and N. Trcera, Phys. Rev. B 85 (2012) 224108
[23] O. Bunau and Y. Joly, J. Phys. Condens. Matter 21 (2009) 345501
[24] J. Stöhr "NEXAFS Spectroscopy" Springer 1996
[25] V. Ilakovac, N. B. Brookes, J. Criginski Cezar, P. Thakur, V. Bisogni, C. Dallera, G. Ghiringhelli, L. Braicovich, S. Bernu, H. Berger, L. Forró, A. Akrap and C. F. Hague, J. Phys.: Condens. Matter 24 (2012) 045503
[26] T. Graf, D. Mandrus, J. M. Lawrence, J. D. Thompson, P. C. Canfield, S. W. Cheong and L. W. Jr. Rupp, Phys. Rev. B 51 (1995) 2037
[27] S. Mitrovic, P. Fazekas, C. Sondergaard, D. Ariosa, N. Barišić, H. Berger, D. Cloetta, L. Forró, H. Hochst, I. Kupčić, D. Pavuna, and G. Margaritondo, Phys. Rev. B 75 (2007) 153103
[28] I. Kézsmárki, G. Mihály, R. Gaál, N. Barišić, A. Akrap, H. Berger, Forró, C. C. Homes and L. Mihály, Phys. Rev. Lett. 96 (2006) 186402
[29] T. Ivek, T. Vuletić, S. Tomić, A. Akrap, H. Berger and L. Forró, Phys. Rev. B 78 (2008) 035110
[30] V. Ilakovac, M. Guarise, M. Grioni, T. Schmitt, K. Zhou, L. Braicovich, G. Ghiringhelli, V. N. Strocov and H. Berger, J. Phys.: Condens. Matter 25 (2013) 505602
[31] F. Sayetat, M. Ghedira, J. Chenavas and M. Marezio, J. Phys. C: Solid State Phys., 15 (1982) 1627
[32] Recent structural refinements, reported by A. Arakcheeva et al. in this Proceedings, point to a new structural transition at 130 K which can be responsible for the semicondutcing behavior below this temperature.